Accelerated propagation modelling for indoor UWB applications

Conor Brennan and John Diskin
The RINCE Institute
Dublin City University
Ireland Email: brennanc@eeng.dcu.ie

Abstract—**Asymptotic solutions which geometrically trace dominant energy paths in the form of rays are an established technique for efficiently modelling wireless propagation in large scale indoor and outdoor environments. A significant computational burden associated with existing frequency domain ray tracing simulators when applied to modelling an Ultra-Wideband (UWB) channel of several Giga-Hertz is the necessity to model the channel at many frequency points. In this paper an acceleration algorithm is described that improves the efficiency of such simulators by approximating the frequency domain response of each individual ray in terms of an analytic rapidly varying portion and a portion which varies slowly with frequency and consequently needs only be computed at a reduced set of frequency points. Results show time savings up to 75% with a maximum relative error in the region of 0.8%.**

I. Introduction

The sanctioning of Ultra-Wideband (UWB) as a wireless communications medium by the Federal Communication Commission (FCC), constitutes a potential for development of novel capabilities in wireless applications [1]. In particular the large bandwidth associated with UWB offers unprecedented data-rates and the possibility of indoor wireless geo-location [2]. In both cases accurate knowledge of the radio channel is necessary. The accurate modelling of EM wave propagation in complex environments constitutes a challenging problem and ray-tracing has been proven to be a popular solution that offers a compromise between accuracy and speed [3]. Its computational speed stems from the fact that it is an asymptotic method, modelling only dominant paths, which also explains why it is not as accurate as full-wave models which still remain computationally impossible for realistic indoor environments. Ray-tracing is most often applied in the frequency domain and can thus be readily extended to model UWB wireless systems. However the need to sample at many frequencies over a wide bandwidth becomes computationally arduous when one considers UWB systems [4]. Instead some practitioners choose to apply time-domain ray tracing techniques [5]. However these techniques cannot readily include the variations of material properties over the extensive UWB bandwidth. Instead this paper documents work carried out on an acceleration algorithm that reduces the computation associated with frequency domain ray-tracing while still accounting for the effects of frequency dependant material properties. In addition, a comparison of a ray tracing simulation with empirical measurements for an indoor UWB channel is presented.

II. Ray Tracing in frequency domain

In ray-tracing geometric techniques such as image theory are used to identify piecewise linear paths by which dominant energy contributions propagate from transmitter to receiver. Associated with each such path or ray is an electric field which accounts for the phase along the ray, free space attenuation and reflection, diffraction and transmission loss as well as antenna effects. At a point $\mathbf{r}$ the electric field can be written as the sum of the contributions from a discrete set of such rays,

$$\mathbf{E}\left(\mathbf{r},\omega\right)=\sum_{n=1}^{N}\mathbf{R}_{n}\left(\mathbf{r},\omega\right), \qquad (1)$$

where N is the total number of rays from source to receiver, in practice limited by capping the maximum number of scattering events (e.g. reflections) that are permitted within the implementation. The variation of the electric field with frequency in equation (1) is due to the frequency dependency of each ray, which in turn is due to two main factors.

One contribution to frequency dependence is due to the total path length traversed by the ray which results in different electrical lengths for each frequency. Although this results in a phase component that varies rapidly with frequency, the effect can be easily computed in situations where one has accurate information about the environment.

In addition one can attribute additional frequency dependent effects to antenna effects, interactions of each ray with scatterers in the propagation environment etc. Transmission, diffraction and reflection coefficients associated with such objects' surfaces undergo variations due to the frequency dependance of the dielectric properties of the constituent material which contribute to variations in the resultant ray. Such effects, while significant and important to model correctly, typically vary slowly with frequency. An example is given in figure (1) which shows the variation in reflection coefficient with frequency for a specific configuration involving reflection from the front face of a concrete slab. The technique presented below separates these frequency dependency behaviours for each ray. Fast variations are extracted and the remaining slowly varying variations are approximated using a low order polynomial specified using explicit numerical calculations performed on a coarsely sampled set of discrete frequencies.

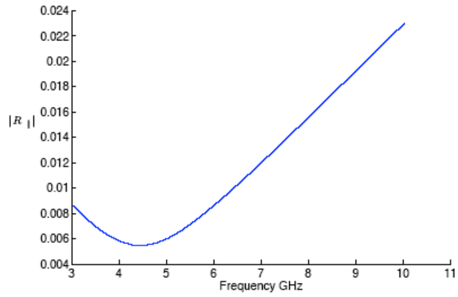

Fig. 1. Variation of parallel reflection coefficient with frequency at incident angle 63°

III. Phase Extraction Technique

A channel response at a point $\mathbf{r}$ can be written as

$$H(\mathbf{r}, \omega) = \sum_{n=1}^{N} R_n(\mathbf{r}, \omega), \tag{2}$$

where $H(\mathbf{r}, \omega)$ is the component of electric field at the point $\mathbf{r}$ in a direction determined by the polarisation of the receiver antenna and R_n is the component of each ray in that direction (incorporating suitable antenna effects). This quantity must be computed for many frequency points ω_1 to ω_Q where Q is sufficiently large to ensure a satisfactory sampling rate. It is this need to sample finely in frequency that leads to an arduous computational burden when applying these techniques to UWB. The proposed acceleration technique reduces the amount of frequency samples that must be explicitly computed by explicitly separating the fast and slow varying components of each ray. Suppressing the positional dependence $\mathbf{r}$ equation (2) is rewritten as

$$H(\omega) = \sum_{n=1}^{N} A_n(\omega) e^{-\jmath\phi_n(\omega)}, \tag{3}$$

where A_n and ϕ_n are the amplitude and phase associated with each ray contribution and which are both frequency dependent. The phase contribution can be further factorised to yield

$$H(\omega) = \sum_{n=1}^{N} A_n(\omega) e^{-\jmath\tilde{\phi}_n(\omega)} e^{-\jmath\phi_n^{(d)}(\omega)}, \tag{4}$$

where $\phi_n^{(d)}$ is the phase behaviour associated with the free-space propagation of the ray and $\tilde{\phi}_n$ is a residual phase behaviour associated with other effects such as reflections, transmissions and diffractions along the ray. The free-space phase term $\phi_n^{(d)}$ has the simple form

$$\phi_n^{(d)}(\omega) = \frac{d_n \omega}{c}, \tag{5}$$

where d_n is the free-space path length of the ray and c is the speed of light in a vacuum. By dividing out this linear phase, a slowly varying term $A_n(\omega) e^{-\jmath\tilde{\phi}_n(\omega)}$ remains. Consequently this residual can be approximated by P_n, a low order polynomial of order m, i.e.

$$A_n(\omega) e^{-\jmath\tilde{\phi}_n(\omega)} \simeq P_n(\omega) \tag{6}$$

which yields the approximate channel response

$$H(\omega) \simeq \sum_{n=1}^{N} e^{-\jmath\phi_n^{(d)}(\omega)} P_n(\omega). \tag{7}$$

P_n can be completely specified for each ray by computing exactly the channel response at $m+1 \ll Q$ frequency points. A received signal $r(t)$ can be obtained by multiplying the channel response by $S(\omega)$, the Fourier transform of the transmitted signal $s(t)$, and taking an inverse Fourier transform,

$$r(t) = \mathcal{F}^{-1}(S(\omega) H(\omega)). \tag{8}$$

Note that Q samples are needed to perform this FFT accurately, however now H can be rapidly evaluated at Q sample points by using the polynomial representation P_n and multiplying by the free-space phase term. Alternatively [8] an completely analytic expression for the received signal can be derived by noting that the free-space phase $\phi_n^{(d)}$ corresponds to a delay of $\frac{d_n}{c}$ in the time domain and by using the following Fourier transform identity which allows inversion of product terms in (8) involving powers of ω (from P_n) and $S(\omega)$

$$\mathcal{F}^{-1}\{\left(\frac{\omega}{2\pi}\right)^m S(\omega)\} = \frac{d^m s(t)}{dt^m} \tag{9}$$

A. Excess phase due to propagation through walls

Transmissions through wall-slabs with complex varying permittivities results in a ray undergoing an additional frequency dependent effect. Propagation through such objects results in an additional phase component ϕ^t being added to the frequency domain response of a ray. This component can be expressed as (assuming no multiple interaction within the wall-slab)

$$\phi^t = d_l \beta_l, \tag{10}$$

where d_l is the propagation distance of the ray inside the wall and β_l is the phase constant due to the material given by,

$$\beta_l = \omega\sqrt{\mu\varepsilon'}\{\frac{1}{2}[\sqrt{1+p_e}+1]\}^{\frac{1}{2}}. \tag{11}$$

where μ is the permeability, ε' is relative permittivity and p_e is the loss tangent of the wall's constituent material. The total phase of a ray that propagates through an air medium and a single wall can thus be expressed as

$$\phi_n^{tot}(\omega) = \frac{d_n \omega}{c} + d_l \beta_l \tag{12}$$

While $\phi_n^{tot}(\omega)$ is not a linear phase response it can be approximated by an effective linear phase $\phi_n^e \approx \phi_n^{tot}$. This is possible as the portion of a typical ray that passes through a wall slab in an indoor environment will be significantly shorter than the free-space propagation length such that $d_n \gg d_l$. The effective linear phase ϕ_n^e can thus be used in equation (4) instead of ϕ_n^d as a means of isolating the slowly varying residuals.

IV. Results

In order to evaluate the accuracy and efficiency of the proposed algorithm a ray tracing simulation was performed in a room mock-up based on the layout of the Sensor Laboratory of the Antennas and Electromagnetic Research Group at Queen Mary University London (Figure 2). For the purposes of our simulations, we use the values of the relative complex permittivity for concrete as measured by Muqaibel et al in [6] (See Figure 3). In this simple example rays were limited to two orders of reflection and the transmitted signal $s(t)$ consisted of a Gaussian doublet pulse waveform of Equation 13, as shown in Figures 4 and 5.

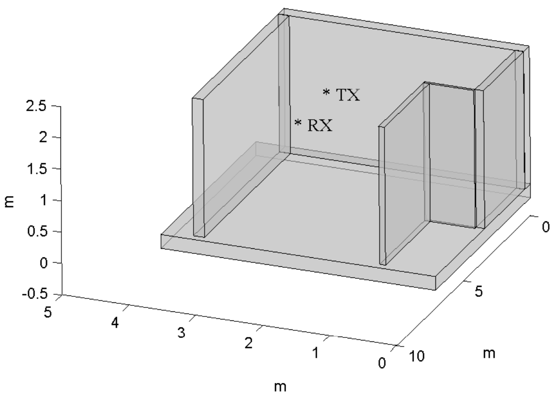

Fig. 2. Building environment used for simulations and measurements

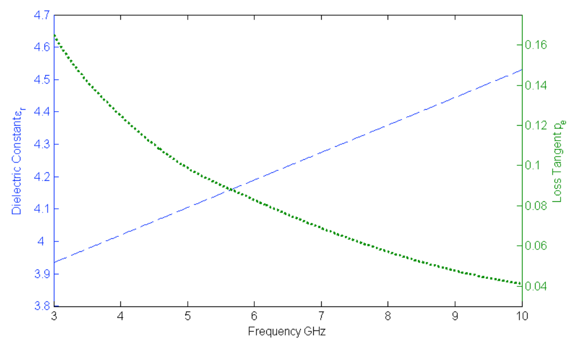

Fig. 3. Variation of electrical parameters of concrete with frequency from [6]

$$s\left(t\right)=1-\left(4\pi\left(\frac{t}{t_n}\right)^2\right)\exp\left(-2\pi\left(\frac{t}{t_n}\right)^2\right), \tag{13}$$

where $t_n = 0.780$ nanoseconds a parameter which determines the bandwidth of the pulse. A ray trace simulation was carried out over a full set of 800 frequency samples from 0.5 MHz to 10 GHz. Subsequently a simulation using a reduced frequency sweep and 10^{th} order polynomials was used to approximate the individual ray responses in the frequency domain. Figure 6 shows a section of the time domain received signal $r(t)$ at a point obtained using the accelerated technique along side the received signal computed using the original full frequency sweep ray-trace. From Figure 6 it is clear that the full frequency sweep simulation results match those of the accelerated reduced frequency sweep in the time domain. This is confirmed in Figure 7 where the relative error between the two time-domain signals is displayed. A relative error of less than 0.8% is observed. It should be noted that by applying the acceleration algorithm a 75% time saving was achieved in the time required to process the rays over the frequency range (the time required to identify the rays remains the same, and can be tackled using suitable visibility algorithms). Further simulations have shown savings of 30% to 40% for more complicated propagation environments including transmission.

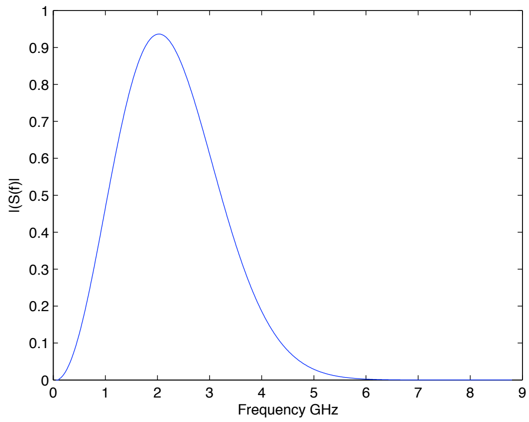

Fig. 4. Gaussian Doublet transmitted UWB Pulse

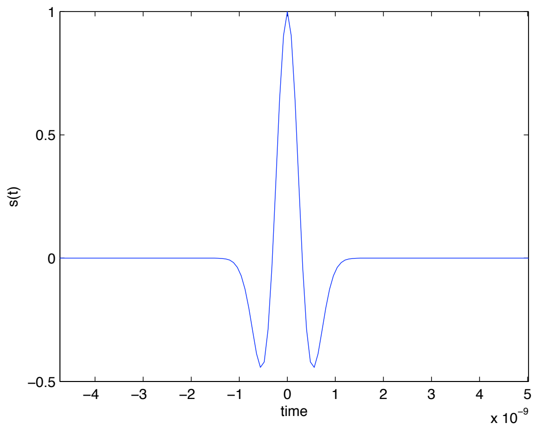

Fig. 5. Gaussian doublet Pulse in time domain

In order to access the accuracy of our simulator a measurement campaign was conducted. which measuring the channel impulse response of a UWB channel at a grid of points in the building environment shown in Figure 2. A UWB channel bandwidth from 3 GHz to 10 GHz was used and

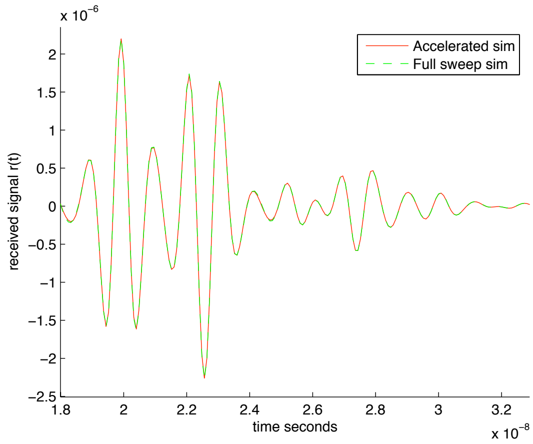

Fig. 6. Original Time Domain Channel Response and Channel Response obtained using 10^{th} order approximation, Full line (red): Approximated Channel, Dashed line (green): Full simulated Channel

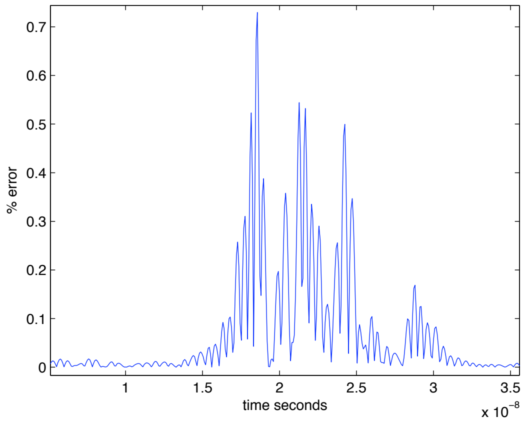

Fig. 7. Relative error of reduced order approximation versus full simulation

Planar Inverted Cone Antenna (PICA) developed at Queen Mary University London [7] were used as transmitters and receivers respectively. This measured impulse response (green) is shown in Figure 8 along with simulated response (red). The transmitter-receiver antenna pair was positioned 2.1 meters apart as in Figure 2. The antenna gain patterns used in the simulation were provided by QMUL at a discrete set of frequency points in the UWB range and interpolation was used to approximate patterns at intermediate frequencies.

V. Conclusion

A frequency domain based ray tracing acceleration technique has been described that reduces the number of frequency samples at which a ray trace has to be processed when simulating UWB propagation. Deploying this accelerated simulator in a indoor building scenario yields a time saving of up to 75% with no visible degradation in the computed time-domain fields. Additionally, validation of simulation result with empirical measurements has been performed which suggests reasonable agreement. Future work will concentrate on

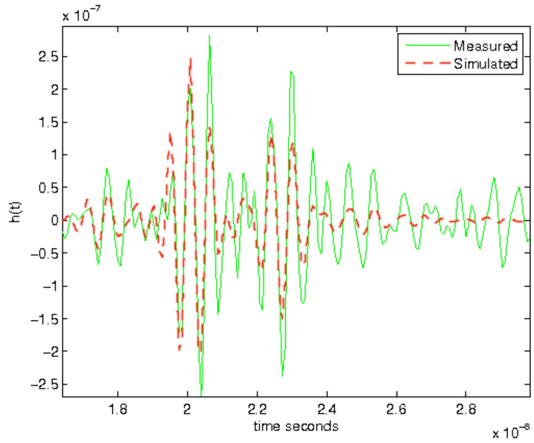

Fig. 8.

using the time-domain simulation capability to increase the efficiency of indoor location systems based on UWB.

VI. Acknowledgements

The authors would like to acknowledge the contribution of the Department of Electrical Engineering, Trinity College Dublin, and in particular Dr. Eamonn Kenny who developed the narrow band version of the ray tracing program. Financial support from the Irish Research Council for Science Engineering and Technology is gratefully acknowledged.

References

[1] Porcino, P. and W. Hirt, "Ultra-wideband Radio Technology: potential and challenges ahead,"*IEEE Communications Magazine*, Vol. 41, No. 7, 66-74, 2003.

[2] Tian, Z., G B. Giannakis, H. Kobayashi, A. F. Molisch, V. H. Poor and Z. Sahinoglu, "Localization via ultra-wideband radios: A look at positioning aspects of future sensor networks," IEEE Signal Processing Magazine, Vol. 22, n 4, p 70-84, July 2005.

[3] Kim, S. C., B. J. Guarino Jr, T. M. Willis III, E. Vinko,S. J. Fourtune, R. A. Valenzuela et al, "Radio propagation measurements and prediction using three-dimensional ray tracing in urban environments at 908 MHz and 1.9 GHz," IEEE Transactions on Vehicular Technology, Vol. 48, No. 3, 931-945, 1999.

[4] Diskin, J. and C. Brennan, "A 3D Ray Tracing Tool for Indoor UWB Signal Propagation Modelling," *Proceedings of the IEE Irish Signals and Systems Conference 2005*, Dublin, Ireland, September 2005, 289-93.

[5] Yao, R., W. Zhu and Z. Chen, "An Efficient Time-Domain Ray Model for UWB Indoor Multipath Propagation Channel," *Proceedings of the 2003 IEEE 58th Vehicular Technology Conference VTC 2003-Fall*, Orlando, United Stated, Vol.2 , Pt. 2, 2003, 1293-7.

[6] Muqaibel, A., A. Safaai-Jazi, A. Bayram, A.M. Attiya and S.M. Riad, "Ultrawideband through-the-wall propagation," *IEE Proceeding.Microwave and Antennas Propagation*, Vol. 152, No. 6, December 2005.

[7] Alomainy, A., Y. Hao, C. G. Parini, and P. S. Hall, "Comparison Between Two Different Antennas for UWB On-Body Propagation Measurements," *IEEE Antennas and Wireless Propagation Letters*, Vol. 4, 2005.

[8] J. Diskin, A. Alomainy and C. Brennan, An accelerated frequency-domain ray tracing simulator for Ultra-wideband communications, *PIERS* March 23-27 2009, Beijing, China